Stochastic Models for Chemically Reacting Systems Using Polynomial Stochastic Hybrid Systems⋆

João Pedro Hespanha and Abhyudai Singh⋆⋆

Center for Control Engineering and Computation
University of California, Santa Barbara, CA 93101
Email:hespanha@ece.ucsb.edu, abhi@engineering.ucsb.edu

Abstract. A stochastic model for chemical reactions is presented, which represents the population of various species involved in a chemical reaction as the continuous state of a *polynomial* Stochastic Hybrid System (pSHS). pSHSs correspond to stochastic hybrid systems with polynomial continuous vector fields, reset maps, and transition intensities. We show that for pSHSs, the dynamics of the statistical moments of its continuous states, evolves according to infinite-dimensional linear ordinary differential equations (ODEs), which can be approximated by finite-dimensional nonlinear ODEs with arbitrary precision. Based on this result, a procedure to build this types of approximation is provided.

This procedure is used to construct approximate stochastic models for a variety of chemical reactions that have appeared in literature. These reactions include a simple bimolecular reaction, for which one can solve the master equation; a decaying-dimerizing reaction set which exhibits two distinct time scales; a reaction for which the chemical rate equations have a continuum of equilibrium points; and the bistable Schögl reaction. The accuracy of the approximate models is investigated by comparing with Monte Carlo simulations or the solution to the Master equation, when available.

1 Introduction

The time evolution of a spatially homogeneous mixture of chemically reacting molecules is often modeled using a stochastic formulation, which takes into account the inherent randomness of thermal molecular motion. This formulation is superior to the traditional deterministic formulation of chemical kinetics and is motivated by complex reactions inside living cells, where small populations of key reactants can set the stage for significant stochastic effects [1–3]. Although most of the mathematical modeling of genetic networks represents gene expression and regulation as deterministic processes, recent observations of gene expression in individual cells illustrate the stochastic nature of transcription [4, 5]. Furthermore, studies of engineered genetic circuits designed to act as toggle switches or oscillators have revealed large stochastic effects [2, 6]. Stochastically is therefore an inherent feature of biological dynamics and developing stochastic models which capture this stochastically have become increasingly important.

In the stochastic formulation, the time evolution of the system is described by a single equation for a grand probability function, where time and species populations appear as independent variables, called the Master equation [7]. However, this equation can only be solved for relatively few, highly idealized cases and generally Monte Carlo simulation techniques are used which are also known as the Stochastic Simulation Algorithm (SSA) [8–11]. Since one is often interested in only the first and second order moments for the number of molecules of the different species involved, much effort can be saved by applying approximate methods to produce these low-order moments, without actually having to solve for the probability density function. Various such approximate methods have been developed, for example, using the Fokker-Plank approximation, expanding the Master equation, etc. [7]. In this paper, an alternative approximate method for

estimating lower-order moments is introduced, by representing the dynamics of a chemical reaction as a Stochastic Hybrid System (SHS).

Hybrid systems are characterized by a state-space that can be partitioned into a continuous domain (typically $\mathbb{R}^n$) and a discrete set (typically finite). In Stochastic Hybrid systems (SHS), both components of the state are stochastic processes, with the evolution of the continuous-state determined by a stochastic differential equation (SDE) and a transition or reset map. Each time a transition is "activated," the SHS's state is updated according to the reset map. The rate at which these "activations" occur, may depend on the overall state. A formal definition for this SHS model, which was taken from [12], can be found in Sec. 2. Polynomial stochastic hybrid systems (pSHSs) arise when the continuous vector fields in the SDE, the reset maps, and the transition intensities are all polynomial functions of the continuous state.

In this paper we show that the evolution of the populations of several species involved in a set of chemical reactions can be modelled by a SHS. Each reaction corresponds to a reset map defined by its stoichiometry, which is activated at a rate determined by the reaction rate. In fact, we show in Sec. 2 that molecular reactions can actually be modelled by pSHSs. An important property of pSHSs is that, if one creates an infinite vector containing the probabilities of all the statistical moments of the continuous state, the dynamics of this vector are governed by an infinite-dimensional linear ordinary differential equation (ODE), which we call the *infinite-dimensional moment dynamics* and define formally in Sec. 3.

In general, the infinite-dimensional *linear* ODEs that describe the moment dynamics for pSHSs are still not easy to solve analytically, and solving them would be essentially equivalent to solving the Master equation. However, they can be accurately approximated by a finite-dimensional *nonlinear* ODE, which we call the *truncated moment dynamics.* The state of this *truncated moment dynamics* typically contains the lower-order moments of interest. We show in Sec. 3 that, under suitable stability assumptions, it is in principle possible for a finite-dimensional nonlinear ODE to approximate the infinite-dimensional moment dynamics, up to an error that can be made arbitrarily small. A procedure to actually construct these finite-dimensional approximations is outlined in Sec. 4.

These finite-dimensional ODE's provide time evolution of lower order moments for populations of species involved in a chemical reaction. Apart from providing fast simulation times and lesser computation burden compared to Monte Carlo simulations these approximate models also open the doors to other types of analysis tools, for example, sensitivity analysis of chemical master equation [13]. However, they provide lesser information about the probability distribution as compared to Monte Carlo simulations, for example, these approximate models do not provide information about time correlations.

To illustrate the applicability of the results we consider several systems that have appeared in the literature. For each example, we construct in Sec. 5 truncated moment dynamics and evaluate how they compare with estimates for the moments obtained from a large number of Monte Carlo simulations which are carried using the SSA. The examples considered here are as follows:

1. A simple bimolecular reaction, for which one can actually compute the first and second order moments directly from the Master equation [14]. The exact results are compared to their estimates from the truncated model.
2. A decaying-dimerizing reaction set [9, 15]. This reaction is difficult to simulate due to the existence of two very distinct time scales and methods that do not require Monte Carlo simulations are of special interest.
3. A reaction for which the deterministic chemical rate equations have a continuum of equilibrium points. This reaction was selected as an example because the approximate methods developed in [7], are not applicable.
4. The Schögl reaction [16]. This reaction is particularly interesting as the deterministic chemical rate equations are bistable, i.e., have two stable equilibrium points for particularly chosen reaction rates.

2 Polynomial Stochastic Hybrid Systems

A SHS is defined by a stochastic differential equation (SDE)

$$\dot{\mathbf{x}} = f(\mathbf{q}, \mathbf{x}, t) + g(\mathbf{q}, \mathbf{x}, t)\dot{\mathbf{w}}, \qquad f : \mathcal{Q} \times \mathbb{R}^n \times [0, \infty) \to \mathbb{R}^n, \quad g : \mathcal{Q} \times \mathbb{R}^n \times [0, \infty) \to \mathbb{R}^{n \times k}, \qquad (1)$$

a family of m *discrete transition/reset maps*

$$(\mathbf{q}, \mathbf{x}) = \phi_\ell(\mathbf{q}^-, \mathbf{x}^-, t), \qquad \phi_\ell : \mathcal{Q} \times \mathbb{R}^n \times [0, \infty) \to \mathcal{Q} \times \mathbb{R}^n, \quad \forall \ell \in \{1, \dots, m\}, \qquad (2)$$

and a family of m *transition intensities*

$$\lambda_\ell(\mathbf{q}, \mathbf{x}, t), \qquad \lambda_\ell : \mathcal{Q} \times \mathbb{R}^n \times [0, \infty) \to [0, \infty), \quad \forall \ell \in \{1, \dots, m\}, \qquad (3)$$

where $\mathbf{w}$ denotes a k-vector of independent Brownian motion processes and $\mathcal{Q}$ a (typically finite) discrete set. A SHS characterizes a jump process $\mathbf{q} : [0, \infty) \to \mathcal{Q}$ called the *discrete state*; a stochastic process $\mathbf{x} : [0, \infty) \to \mathbb{R}^n$ with piecewise continuous sample paths called the *continuous state*; and m stochastic counters $\mathbf{N}_\ell : [0, \infty) \to \mathbb{N}_{\geq 0}$ called the *transition counters*. In essence, between transition counter increments the discrete state remains constant whereas the continuous state flows according to (1). At transition times, the continuous and discrete states are reset according to (2). Each transition counter $\mathbf{N}_\ell$ counts the number of times that the corresponding discrete transition/reset map ϕ_ℓ is "activated." The frequency at which this occurs is determined by the transition intensities (3). In particular, the probability that the counter $\mathbf{N}_\ell$ will increment in an "elementary interval" $(t, t+dt]$, and therefore that the corresponding transition takes place, is given by $\lambda_\ell(\mathbf{q}(t), \mathbf{x}(t), t)dt$. In practice, one can think of the intensity of a transition as the instantaneous rate at which that transition occurs. Expectations of the state of a SHS can be computed using the following result from [12].

Theorem 1. *For every function $\psi : \mathcal{Q} \times \mathbb{R}^n \times [0, \infty) \to \mathbb{R}$ that is continuously differentiable with respect to its second and third arguments, we have that*

$$\frac{d \, \mathrm{E}[\psi(\mathbf{q}(t), \mathbf{x}(t), t)]}{dt} = \mathrm{E}[(L\psi)(\mathbf{q}(t), \mathbf{x}(t), t)], \qquad (4)$$

where $\forall(q, x, t) \in \mathcal{Q} \times \mathbb{R}^n \times [0, \infty)$

$$(L\psi)(q, x, t) := \frac{\partial \psi(q, x, t)}{\partial x} f(q, x, t) + \frac{\partial \psi(q, x, t)}{\partial t} +$$

$$+ \frac{1}{2} \operatorname{trace}\left(\frac{\partial^2 \psi(q, x)}{\partial x^2} g(q, x, t) g(q, x, t)'\right) + \sum_{\ell=1}^m \left(\psi(\phi_\ell(q, x, t), t) - \psi(q, x, t)\right) \lambda_\ell(q, x, t), \quad (5)$$

and $\frac{\partial \psi(q, x, t)}{\partial t}$, $\frac{\partial \psi(q, x, t)}{\partial x}$, and $\frac{\partial^2 \psi(q, x)}{\partial x^2}$ denote the partial derivative of $\psi(q, x, t)$ with respect to t, the gradient of $\psi(q, x, t)$ with respect to x, and the Hessian matrix of ψ with respect to x, respectively. The operator $\psi \mapsto L\psi$ defined by (5) is called the extended generator *of the SHS.* $\square$
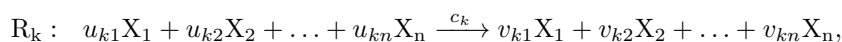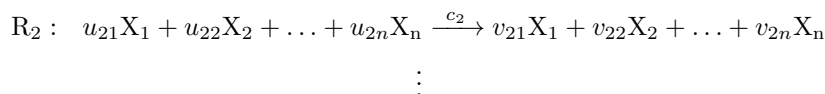
We say that a SHS is *polynomial (pSHS)* if its extended generator L is closed on the set of finite-polynomials in x, i.e., $(L\psi)(q, x, t)$ is a finite-polynomial in x for every finite-polynomial $\psi(q, x, t)$ in x. By a *finite-polynomials in x* we mean a function $\psi(q, x, t)$ such that $x \mapsto \psi(q, x, t)$ is a (multi-variable) polynomial of finite degree for each fixed $q \in \mathcal{Q}$, $t \in [0, \infty)$. A pSHS is obtained, e.g., when the vector fields f and g, the reset maps ϕ_ℓ, and the transition intensities λ_ℓ are all finite-polynomials in x.

It turns out that sets of chemical reactions can be represented by such a pSHS. To understand why this is so, consider n species $X_1, X_2, \dots, X_n$ inside a fixed volume V involved in a system of k reactions R_1, R_2, $\dots$, R_k of the form

$$R_1 : \quad u_{11}X_1 + u_{12}X_2 + \dots + u_{1n}X_n \xrightarrow{c_1} v_{11}X_1 + v_{12}X_2 + \dots + v_{1n}X_n$$

3
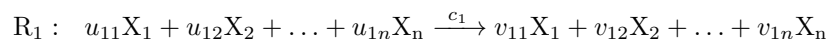
Table 1. h_i and c_i for different reaction types.

Reaction R_i	h_i	c_i
$X_i \rightarrow$ reaction products	$\mathbf{x}_i$	k_i
$X_i + X_j \rightarrow$ reaction products, $\quad (i \neq j)$	$\mathbf{x}_i \mathbf{x}_j$	$\frac{k_i}{V}$
$2X_i \rightarrow$ reaction products	$\frac{1}{2}\mathbf{x}_i(\mathbf{x}_i - 1)$	$\frac{2k_i}{V}$
$X_i + 2X_j \rightarrow$ reaction products, $\quad (i \neq j)$	$\frac{1}{2}\mathbf{x}_i \mathbf{x}_j(\mathbf{x}_j - 1)$	$\frac{2k_i}{V^2}$
$3X_i \rightarrow$ reaction products	$\frac{1}{6}\mathbf{x}_i(\mathbf{x}_i - 1)(\mathbf{x}_i - 2)$	$\frac{6k_i}{V^2}$

$$R_2: \quad u_{21}X_1 + u_{22}X_2 + \ldots + u_{2n}X_n \xrightarrow{c_2} v_{21}X_1 + v_{22}X_2 + \ldots + v_{2n}X_n$$

$$\vdots$$

$$R_k: \quad u_{k1}X_1 + u_{k2}X_2 + \ldots + u_{kn}X_n \xrightarrow{c_k} v_{k1}X_1 + v_{k2}X_2 + \ldots + v_{kn}X_n,$$

where u_{ij} is the stoichiometry associated with the jth reactant of the ith reaction and v_{ij} is the stoichiometry associated with the jth product of the ith reaction. The reaction parameter c_i characterizes the reaction R_i and, together with the stoichiometry, defines the probability that a particular reaction takes place in an "infinitesimal" time interval $(t, t + dt]$. This probability is given by the product of the following two terms:

1. the number h_i of distinct molecular reactant combinations present in V at time t for the reaction R_i,
2. the probability $c_i dt$ that a particular combination of R_i reactant molecules will actually react on $(t, t+dt]$.

In general, h_i depends both on the reactants stoichiometry u_{ij} in R_i and on the number of reactant molecules in V. Table 1 shows the value of h_i for different reaction types [8]. In this table and in the sequel, we denote by $\mathbf{x_i}$ the number of molecules of the species X_i in the volume V. The reaction parameter c_i is related to the reaction rate k_i in the deterministic formulation of chemical kinetics by the formulas shown in the right-most column of Table 1.

The evolution of the number of molecules $\mathbf{x}_1$, $\mathbf{x}_2$, ..., $\mathbf{x}_n$ can be generated by a pSHS. Since the number of molecules take values in the discrete set on integers, they can be regarded then as either part of the discrete or the continuous state of the pSHS. However, since we are interested in computing the statistical moments of $\mathbf{x}_i$, we chose to view them as part of a continuous state. In this case the SHS has a single discrete mode, which we omit for simplicity. The continuous state consists of a vector $\mathbf{x} := \begin{bmatrix} \mathbf{x}_1, \mathbf{x}_2, \ldots, \mathbf{x}_n \end{bmatrix}'$ with trivial continuous dynamics $\dot{\mathbf{x}} = 0$. Each one of the k reactions is associated with a reset map defined by the stoichiometry

$$\mathbf{x} \mapsto \phi_1(\mathbf{x}) := \begin{bmatrix} \mathbf{x}_1 - u_{11} + v_{11} \\ \mathbf{x}_2 - u_{12} + v_{12} \\ \vdots \\ \mathbf{x}_n - u_{1n} + v_{1n} \end{bmatrix} \quad \mathbf{x} \mapsto \phi_2(\mathbf{x}) := \begin{bmatrix} \mathbf{x}_1 - u_{21} + v_{21} \\ \mathbf{x}_2 - u_{22} + v_{22} \\ \vdots \\ \mathbf{x}_n - u_{2n} + v_{2n} \end{bmatrix} \quad \ldots \quad \mathbf{x} \mapsto \phi_k(\mathbf{x}) := \begin{bmatrix} \mathbf{x}_1 - u_{k1} + v_{k1} \\ \mathbf{x}_2 - u_{k2} + v_{k2} \\ \vdots \\ \mathbf{x}_n - u_{kn} + v_{kn} \end{bmatrix},$$

with transition intensities given by

$$\lambda_1(\mathbf{x}) := c_1 h_1 \qquad\qquad \lambda_2(\mathbf{x}) := c_2 h_2 \qquad\qquad \ldots \qquad \lambda_k(\mathbf{x}) := c_k h_k,$$

respectively. This results in a pSHS because the reset maps and the transition intensities are finite polynomials in $\mathbf{x}_i$.

3 Moment Dynamics

To fully characterize the dynamics of a chemical reaction one would like to determine the evolution of the probability distribution for $\mathbf{x}(t)$, i.e. solve the Master equation. In general, this is difficult and a more reasonable goal is to determine the evolution of a few low-order moments.

Given a vector of n integers $m = (m_1, m_2, \ldots, m_n) \in \mathbb{N}_{\geq 0}^n$, we define the *test-function associated with m* to be $\psi^{(m)}(x) := x^{(m)}$, $\forall x \in \mathbb{R}^n$ and the *(uncentered) moment associated with m* to be

$$\mu^{(m)}(t) := \mathbf{E}\big[\psi^{(m)}\big(\mathbf{x}(t)\big)\big], \qquad \forall t \geq 0. \tag{6}$$

Here and in the sequel, given a vector $x = (x_1, x_2, \ldots, x_n)$, we use $x^{(m)}$ to denote the monomial $x_1^{m_1} x_2^{m_2} \cdots x_n^{m_n}$. pSHSs have the property that if one stacks all moments in an infinite vector μ_∞, its dynamics can be written as

$$\dot{\mu}_\infty = A_\infty(t)\mu_\infty, \qquad \forall t \geq 0, \tag{7}$$

for some appropriately defined infinite matrix $A_\infty(t)$. This is because $\forall m = (m_1, \ldots, m_n) \in \mathbb{N}_{\geq 0}^n$, $(L\psi^{(m)})(x, t)$ is a finite-polynomial in x and therefore can be written as a finite linear combination of test-functions (possibly with time-varying coefficients). Equation (7) then follows directly from (4), (5), and (6). In the sequel, we refer to (7) as the *infinite-dimensional moment dynamics*.

Since we are only interested in computing a few low-order moments, we rewrite (7) as

$$\dot{\mu} = I_{k \times \infty} A_\infty(t)\mu_\infty = A(t)\mu + B(t)\bar{\mu}, \qquad \bar{\mu} = C\mu_\infty, \tag{8}$$

where $\mu \in \mathbb{R}^k$ contains to the top k elements of μ_∞, which correspond to the lower-order moments of interest. $I_{k \times \infty}$ denotes a matrix composed of the first k rows of the infinite identity matrix, $\bar{\mu} \in \mathbb{R}^r$ contains all the moments that appear in the first k elements of $A_\infty(t)\mu_\infty$ but that do not appear in μ, and C is the projection matrix that extracts $\bar{\mu}$ from μ_∞. Our goal is to approximate the infinite dimensional system (7) by a finite-dimensional nonlinear ODE of the form

$$\dot{\nu} = A(t)\nu + B(t)\bar{\nu}(t), \quad \bar{\nu} = \varphi(\nu, t), \tag{9}$$

where the map $\varphi : \mathbb{R}^k \times [0, \infty) \to \mathbb{R}^r$ should be chosen so as to keep $\nu(t)$ close to $\mu(t)$. We call (9) the *truncated moment dynamics* and φ the *truncation function*. We make the following two stability assumptions to establish sufficient conditions on φ, for the approximation to be valid.

Assumption 1 (Boundedness). *There exist sets $\Omega_\mu \in \mathbb{R}^\infty$ and $\Omega_\nu \in \mathbb{R}^k$ such that all solutions to (7) and (9) starting at some time $t_0 \geq 0$ in Ω_μ and Ω_ν, respectively, exist and are smooth on $[t_0, \infty)$ with all derivatives of their first k elements uniformly bounded by the same constant. The set Ω_ν is assumed to be forward invariant under the dynamics of (9).* $\qquad\square$

Assumption 2 (Incremental Asymptotic Stability). *There exists a function[1] $\beta \in \mathcal{KL}$ such that, for every solution μ_∞ to (7) starting in Ω_μ at some time $t_0 \geq 0$, and every $t_1 \geq t_0$, $\nu_1 \in \Omega_\nu$ there exists some $\hat{\mu}_\infty(t_1) \in \Omega_\mu$ whose first k elements match ν_1 and*

$$\|\mu(t) - \hat{\mu}(t)\| \leq \beta(\|\mu(t_1) - \hat{\mu}(t_1)\|, t - t_1), \qquad \forall t \geq t_1,$$

where $\mu(t)$ and $\hat{\mu}(t)$ denote the first k elements of the solutions to (7) starting at $\mu_\infty(t_1)$ and $\hat{\mu}_\infty(t_1)$, respectively. $\qquad\square$

Let $\frac{d^i \mu(t)}{dt^i}$ and $\frac{d^i \nu(t)}{dt^i}$ represent the ith time derivative of $\mu(t)$ and $\nu(t)$ along the trajectories of system (7) and (9) respectively. The following result from [17] shows that if a sufficiently large but *finite* number of these derivatives match point-wise, then, the difference between solutions to (8) and (9), i.e. $\mu(t)$ and $\nu(t)$ converges to an arbitrarily small ball.

---

[1] A function $\beta : [0, \infty) \times [0, \infty) \to [0, \infty)$ is said to be of *class $\mathcal{KL}$* if $\beta(0, t) = 0$, $\forall t \geq 0$; $\beta(s, t)$ is continuous and strictly increasing on s for each fixed $t \geq 0$; and $\lim_{t \to \infty} \beta(s, t) = 0$, $\forall s \geq 0$.

Theorem 2. *Suppose Assumptions 1 and 2 hold. Then, for every $\delta > 0$, there exists an integer N, sufficiently large, for which the following result holds: Assuming that for every $t_0 \geq 0$, $\mu_\infty(t_0) \in \Omega_\mu$, $\nu(t_0) \in \Omega_\nu$*

$$\mu(t_0) = \nu(t_0) \Rightarrow \frac{d^i \mu(t_0)}{dt^i} = \frac{d^i \nu(t_0)}{dt^i}, \quad \forall i \in \{1, \ldots, N\} \tag{10}$$

where μ is the first k elements of μ_∞. Then,

$$\|\mu(t) - \nu(t)\| \leq \delta, \ \forall t \in [t_0, \infty) \tag{11}$$

along solutions of (7) *and* (9). □

For the problems considered in this paper, Assumptions 1 and 2 are hard to verify. Moreover, given a constant $\delta > 0$ and sets Ω_μ, Ω_ν, it is generally difficult to determine the integer N for which the bound (11) holds. Nevertheless, Theorem 2 is still useful because it provides the explicit conditions (10) that the truncation function φ should satisfy for the solution to the truncated system to approximate the one of the original system. In the subsequent section we use (10) for $N = 2$ to explicitly compute φ.

4 Construction of Approximate Truncations

In this section, we compute the truncation function φ by requiring (10) to hold for $N = 2$. Using (8) and (9), equality (10) reduces to

$$\mu(t_0) = \nu(t_0) \Rightarrow \bar{\mu}(t_0) = \varphi(\mu(t_0), t_0) \qquad (i = 1) \tag{12}$$

$$\mu(t_0) = \nu(t_0) \Rightarrow \frac{d\bar{\mu}(t)}{dt}\Big|_{t=t_0} = \frac{\partial \varphi(\mu(t_0), t_0)}{\partial \mu} I_{k \times \infty} A_\infty(t_0) \mu_\infty(t_0) + \frac{\partial \varphi(\mu(t), t)}{\partial t}\Big|_{t=t_0} \quad (i = 2). \tag{13}$$

We look for solutions to the PDE (13) having the following separable form

$$\varphi(\nu, t) = \nu^{(\Gamma)} := \begin{bmatrix} \nu_1^{\gamma_{11}} \nu_2^{\gamma_{12}} \cdots \nu_k^{\gamma_{1k}} \\ \nu_1^{\gamma_{21}} \nu_2^{\gamma_{22}} \cdots \nu_k^{\gamma_{2k}} \\ \vdots \\ \nu_1^{\gamma_{r1}} \nu_2^{\gamma_{r2}} \cdots \nu_k^{\gamma_{rk}} \end{bmatrix},$$

for an appropriately chosen constant matrix $\Gamma := [\gamma_{ij}] \in \mathbb{R}^{r \times k}$. In order to compute Γ, we take Ω_μ to be the set that corresponds to the family of deterministic distributions. For this set, $\mu^{(m)} := x^{(m)}$ and a necessary condition determined in [17] for the existence of a matrix Γ that satisfies (12) and (13) is that, for every moment $\mu^{(m_\ell)}$ in $\bar{\mu}$, the polynomial $\sum_{i=1}^{\infty} a_{\ell,i} x^{(m_i)}$ must belong to the linear subspace generated by the polynomials[2]

$$\left\{ \sum_{i=1}^{\infty} a_{j,i} x^{(m_\ell - m_j + m_i)} : 1 \leq j \leq k \right\}, \tag{14}$$

where $a_{\ell,i}$ denotes the entry in the ℓth row and i^{th} column of A_∞.

Although the family of deterministic distributions may seem very restrictive, it provide us with truncations that are accurate even when the system evolves towards "nondeterministic distributions," as will be demonstrated in the next section. When the condition (14) does not hold, one can often drop lower order terms from the right-hand-side of (5) to form a new matrix $\bar{A}_\infty$ that satisfies this condition. This will be demonstrated in some of the examples in Section 5. When the solution φ to (12) and (13) is not unique, a specific φ can be selected by requiring (12) to hold for additional families of distribution, e.g., the family of lognormal distributions.

---

[2] The polynomials in (14) can have both positive and negative powers.

Remark 1. For the class of elementary reactions, i.e, uni- or bi-molecular reactions, sufficient conditions for the existence and uniqueness for the solution φ to (12) and (13) will appear in [18]. More specifically, it has been shown in [18], that given a vector μ containing all the first and second order moments of $\mathbf{x}$, (14) holds, if one drops some second and all first order moments from the second time derivative of μ. This will be valid, as long as these moments are dominated by the fourth order moments of $\mathbf{x}$, which also appear in the second time derivative of μ. Furthermore, *explicit formulas* for φ also appear in [18]. The striking features of these formulas is that the dependence of higher order moments on lower order as given by φ is independent of the reaction parameters, moreover, this dependance is consistent with $\mathbf{x}$ being *lognormally distributed.* □

5 Examples

We now develop truncated models for the moment dynamics of several chemical reactions and discuss how they compare with estimates of moments obtained from averaging a large number of Monte Carlo simulations or the exact solution of the Master equation, when available. All Monte Carlo simulations were carried out using the algorithm described in [12], which is equivalent to SSA [8]. Since the quantities of interest in the stochastic approach are often the first and second order moments, we consider truncation models whose state contains only the first and second order moments for the number of molecules in the species involved in the reaction.

Example 1. Consider the following bi-molecular irreversible reaction [14]:

$$2X_1 \xrightarrow{c} X_2.$$
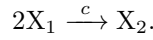
For the sake of simplicity, we omit moments for the population of X_2 from the truncation. The number of molecules $\mathbf{x}$ of X_1, can be generated by a SHS with continuous dynamics $\dot{\mathbf{x}} = 0$ and a reset map

$$\mathbf{x} \mapsto \phi(\mathbf{x}) := \mathbf{x} - 2$$

with intensity $\lambda(\mathbf{x}) := \frac{c}{2}\mathbf{x}(\mathbf{x} - 1)$. For $\psi^{(m)}(x) = x^m$, $\forall m \in \mathbb{N}_{\geq 0}$ we have

$$(L\psi^{(m)})(x) = \frac{c}{2}x(x-1)[(x-2)^m - x^m] = \frac{c}{2}\sum_{i=1}^{m} \binom{m}{i}(x^{m-i+2} - x^{m-i+1})(-2)^i \quad (15)$$

and (8) can be written as follows:

$$\begin{bmatrix} \dot{\mu}^{(1)} \\ \dot{\mu}^{(2)} \end{bmatrix} = \begin{bmatrix} c & -c \\ -2c & 4c \end{bmatrix} \begin{bmatrix} \mu^{(1)} \\ \mu^{(2)} \end{bmatrix} + \begin{bmatrix} 0 \\ -2c \end{bmatrix} \bar{\mu}, \quad (16)$$

where $\bar{\mu} := \mu^{(3)}$ evolves according to

$$\dot{\mu}^{(3)} = -3c\mu^{(4)} + 9c\mu^{(3)} - 10c\mu^{(2)} + 4c\mu^{(1)}.$$

It can be easily verified that for this system, condition (14) is not satisfied, as the polynomial

$$\sum_{i=1}^{\infty} a_{3,i}x^{(m_i)} = -3cx^4 + 9cx^3 - 10cx^2 + 4cx$$

does not belong to the subspace generated by the polynomials

$$\sum_{i=1}^{\infty} a_{1,i}x^{(m_3-m_1+m_i)} = cx^3 - cx^4, \quad \sum_{i=1}^{\infty} a_{2,i}x^{(m_3-m_2+m_i)} = -2cx^2 + 4cx^3 - 2cx^4,$$

due to the first-order term $4cx$. However, if we retain only the two highest powers of x in the summation in the right-hand side of (15), we have the following simplified version of (16)

$$\begin{bmatrix} \dot{\mu}^{(1)} \\ \dot{\mu}^{(2)} \end{bmatrix} = \begin{bmatrix} c & -c \\ 0 & 4c \end{bmatrix} \begin{bmatrix} \mu^{(1)} \\ \mu^{(2)} \end{bmatrix} + \begin{bmatrix} 0 \\ -2c \end{bmatrix} \bar{\mu},$$

Table 2. $E[\mathbf{x}]$ for the exact and approximate truncated models at different times t for Example 1. $E[\mathbf{x}]$ refers to the exact solution, $\mu^{(1)}$ refers to the truncated model (16) and (17) and $\bar{\mu}^{(1)}$ refers to the truncated model developed in [14].

t	$E[\mathbf{x}]$	$\mu^{(1)}$	$\bar{\mu}^{(1)}$
.025	8.15	8.15	8.18
.050	6.86	6.87	6.95
.075	5.93	5.93	6.06
.100	5.21	5.23	5.39
.150	4.21	4.23	4.44

where now $\bar{\mu} := \mu^{(3)}$ evolves according to

$$\dot{\mu}^{(3)} = -3c\mu^{(4)} + 9c\mu^{(3)}$$

for which condition (14) does hold, allowing us to find a unique solution φ to (12) and (13), resulting in a truncated system given by (16) and

$$\bar{\mu} = \varphi(\mu) = \left(\frac{\mu^{(2)}}{\mu^{(1)}}\right)^3. \tag{17}$$

Owing to the simplicity of this reaction, one can obtain the exact solution for $\mu^{(1)} = E[\mathbf{x}]$ and $\mu^{(2)} = E[\mathbf{x}^2]$ from the Master equation, as has been done in [14]. An alternate approximate truncated model, was also developed in [14], where $\mu^{(3)}$ is approximated as $\mu^{(1)}\mu^{(2)}$. Table 2 and Figure 1 compare our estimates for the mean and the coefficient of variation respectively, with that of the exact solution and approximated model developed in [14], for $c = 1$ and initial condition $\mathbf{x}(0) = 10$. Our estimates of $E[\mathbf{x}]$ are almost identical to those of the exact solution, while, those of $CV[\mathbf{x}]$ are close. One can see that the truncation model yields good results for fairly small populations, even though to construct it we dropped lower-order powers of x, which implicitly assumes that the population of the specie X_1 is large. It should be noted that if we retain only the highest powers of x in the summation in the right-hand-side of (15), the unique solution φ to (12) and (13) would have been $\varphi(\mu) = \mu^{(1)}\mu^{(2)}$ as in [14]. As this approximation is obtained by dropping more terms, it is not surprising to discover that it does not perform as well as (17). $\qquad\square$

Example 2. Consider the following decaying-dimerizing reaction set [9, 15]:

$$X_1 \xrightarrow{c_1} 0, \qquad 2X_1 \xrightarrow{c_2} X_2, \qquad X_2 \xrightarrow{c_3} 2X_1, \qquad X_2 \xrightarrow{c_4} X_3.$$

The number of particles $\mathbf{x} := (\mathbf{x}_1, \mathbf{x}_2, \mathbf{x}_3)$ of three species involved in the following set of decaying-dimerizing reaction can be generated by a SHS with continuous dynamics $\dot{\mathbf{x}} = 0$ and four reset maps

$$\mathbf{x} \mapsto \phi_1(\mathbf{x}) := \begin{bmatrix} \mathbf{x}_1 - 1 \\ \mathbf{x}_2 \\ \mathbf{x}_3 \end{bmatrix} \qquad \mathbf{x} \mapsto \phi_2(\mathbf{x}) := \begin{bmatrix} \mathbf{x}_1 - 2 \\ \mathbf{x}_2 + 1 \\ \mathbf{x}_3 \end{bmatrix} \qquad \mathbf{x} \mapsto \phi_3(\mathbf{x}) := \begin{bmatrix} \mathbf{x}_1 + 2 \\ \mathbf{x}_2 - 1 \\ \mathbf{x}_3 \end{bmatrix} \qquad \mathbf{x} \mapsto \phi_4(\mathbf{x}) := \begin{bmatrix} \mathbf{x}_1 \\ \mathbf{x}_2 - 1 \\ \mathbf{x}_3 + 1 \end{bmatrix}$$

with intensities $\lambda_1(\mathbf{x}) := c_1 \mathbf{x}_1$, $\lambda_2(\mathbf{x}) := \frac{c_2}{2} \mathbf{x}_1(\mathbf{x}_1 - 1)$, $\lambda_3(\mathbf{x}) := c_3 \mathbf{x}_2$, and $\lambda_4(\mathbf{x}) := c_4 \mathbf{x}_2$, respectively. The generator for this SHS is given by

$$(L\psi)(x_1, x_2, x_3) = c_1 x_1 \big(\psi(x_1 - 1, x_2, x_3) - \psi(x)\big) + \frac{c_2}{2} x_1(x_1 - 1)\big(\psi(x_1 - 2, x_2 + 1, x_3) - \psi(x)\big)$$
$$+ c_3 x_2 \big(\psi(x_1 + 2, x_2 - 1, x_3) - \psi(x)\big) + c_4 x_2 \big(\psi(x_1, x_2 - 1, x_3 + 1) - \psi(x)\big).$$

Taking $\psi^{(m_1, m_2, m_2)}(x) = x_1^{m_1} x_2^{m_2} x_3^{m_3}$, $\forall m_1, m_2, m_3 \in \mathbb{N}_{\geq 0}$ we have

$$(L\psi^{(m_1, m_2, m_2)})(x) = c_1 x_1 \big((x_1 - 1)^{m_1} - x_1^{m_1}\big) x_2^{m_2} x_3^{m_3} + \frac{c_2}{2} x_1(x_1 - 1)\big((x_1 - 2)^{m_1}(x_2 + 1)^{m_2} - x_1^{m_1} x_2^{m_2}\big) x_3^{m_3}$$
$$+ c_3 x_2 \big((x_1 + 2)^{m_1}(x_2 - 1)^{m_2} - x_1^{m_1} x_2^{m_2}\big) x_3^{m_3} + c_4 x_2 \big((x_2 - 1)^{m_2}(x_3 + 1)^{m_3} - x_2^{m_2} x_3^{m_3}\big) x_1^{m_1}$$

8
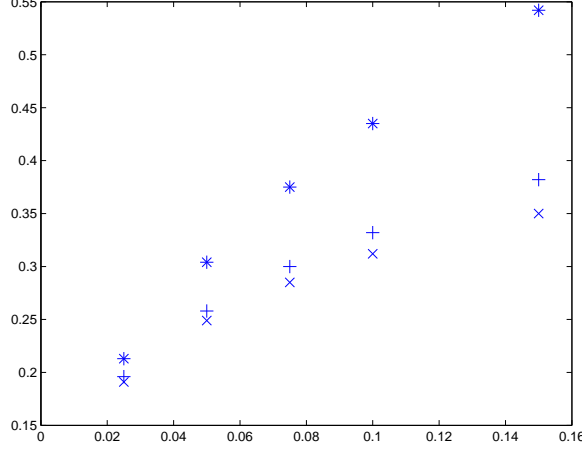
Fig. 1. $CV[\mathbf{x}] = \frac{\sqrt{\mathrm{E}[\mathbf{x}^2] - \mathrm{E}[\mathbf{x}]^2}}{\mathrm{E}[\mathbf{x}]}$ for the exact and approximate truncated models at different times t for Example 1. "+" refers to the exact solution, "×" to the truncated model (16) and (17) and "∗" to the truncated model developed in [14].

$$= c_1 \sum_{i=0}^{m_1-1} \binom{m_1}{i} (-1)^{m_1-i} \psi^{(i+1,m_2,m_3)}(x) + \frac{c_2}{2} \sum_{\substack{i,j=0 \\ (i,j)\neq(m_1,m_2)}}^{m_1,m_2} \binom{m_1}{i}\binom{m_2}{j}(-2)^{m_1-i}\left(\psi^{(i+2,j,m_3)}(x) - \psi^{(i+1,j,m_3)}(x)\right)$$

$$+ c_3 \sum_{\substack{i,j=0 \\ (i,j)\neq(m_1,m_2)}}^{m_1,m_2} \binom{m_1}{i}\binom{m_2}{j}2^{m_1-i}(-1)^{m_2-j}\psi^{(i,j+1,m_3)}(x) + c_4 \sum_{\substack{i,j=0 \\ (i,j)\neq(m_2,m_3)}}^{m_2,m_3} \binom{m_2}{i}\binom{m_3}{j}(-1)^{m_2-i}\psi^{(m_1,i+1,j)}(x),$$

$$(18)$$

where the summations result from the power expansions of the terms $(x_i - c)^{m_i}$. To keep the formulas short, we omit from the truncation the second moments of $\mathbf{x}_3$, which does not appear as a reactant in any reaction and therefore its higher order statistics do not affect the first two. In this case, (8) can be written as follows:

$$
\begin{bmatrix} \dot{\mu}^{(1,0,0)} \\ \dot{\mu}^{(0,1,0)} \\ \dot{\mu}^{(0,0,1)} \\ \dot{\mu}^{(2,0,0)} \\ \dot{\mu}^{(0,2,0)} \\ \dot{\mu}^{(1,1,0)} \end{bmatrix}
=
\begin{bmatrix}
-c_1+c_2 & 2c_3 & 0 & -c_2 & 0 & 0 \\
-\frac{c_2}{2} & -c_3-c_4 & 0 & \frac{c_2}{2} & 0 & 0 \\
0 & c_4 & 0 & 0 & 0 & 0 \\
c_1-2c_2 & 4c_3 & 0 & -2c_1+4c_2 & 0 & 4c_3 \\
-\frac{c_2}{2} & c_3+c_4 & 0 & \frac{c_2}{2} & -2c_3-2c_4 & -c_2 \\
c_2 & -2c_3 & 0 & -\frac{3c_2}{2} & 2c_3 & -c_1+c_2-c_3-c_4
\end{bmatrix}
\begin{bmatrix} \mu^{(1,0,0)} \\ \mu^{(0,1,0)} \\ \mu^{(0,0,1)} \\ \mu^{(2,0,0)} \\ \mu^{(0,2,0)} \\ \mu^{(1,1,0)} \end{bmatrix}
+
\begin{bmatrix} 0 & 0 \\ 0 & 0 \\ 0 & 0 \\ -2c_2 & 0 \\ 0 & c_2 \\ \frac{c_2}{2} & -c_2 \end{bmatrix} \bar{\mu}, \qquad (19)
$$

where $\bar{\mu} := \begin{bmatrix} \mu^{(3,0,0)} & \mu^{(2,1,0)} \end{bmatrix}'$ evolves according to

$$\dot{\mu}^{(3,0,0)} = (-c_1 + 4c_2)\mu^{(1,0,0)} + 8c_3\mu^{(0,1,0)} + (3c_1 - 10c_2)\mu^{(2,0,0)} + 12c_3\mu^{(1,1,0)}$$
$$+ (-3c_1 + 9c_2)\mu^{(3,0,0)} + 6c_3\mu^{(2,1,0)} - 3c_2\mu^{(4,0,0)} \qquad (20a)$$

$$\dot{\mu}^{(2,1,0)} = -2c_2\mu^{(1,0,0)} - 4c_3\mu^{(0,1,0)} + 4c_2\mu^{(2,0,0)} + 4c_3\mu^{(0,2,0)} + (c_1 - 2c_2 - 4c_3)\mu^{(1,1,0)}$$
$$- \frac{5c_2\mu^{(3,0,0)}}{2} + (-2c_1 + 4c_2 - c_3 - c_4)\mu^{(2,1,0)} + 4c_3\mu^{(1,2,0)} + \frac{c_2\mu^{(4,0,0)}}{2} - 2c_2\mu^{(3,1,0)}. \qquad (20b)$$

This system also does not satisfy condition (14) because the $\mu^{(1,0,0)}$, $\mu^{(0,1,0)}$ terms in the right-hand-sides of (20) lead to monomials in x_1 and x_2 in $\sum_{i=1}^{\infty} a_{\ell,i} x^{(m_i)}$ that do not exist in any of the polynomials $\left\{\sum_{i=1}^{\infty} a_{j,i} x^{(m_\ell - m_j + m_i)} : 1 \leq j \leq 6\right\}$. These terms can be easily traced back to the lowest-order terms in power expansions in (18) and disappear if we only keep the three highest powers of x_1 in the expansion of $(x_1 - 1)^{m_1}$ that corresponds to the first reaction and the two highest powers of x_1 and x_2 in the expansions of $(x_1 \pm 2)^{m_1}$ and $(x_2 \pm 1)^{m_2}$ that correspond to the second and third reactions. In practice, this leads to

Table 3. Comparison between estimates obtained from Monte Carlo simulations and the truncated model for Example 2.

Source for the estimates	$\mathrm{E}[\mathbf{x}_1(0.2)]$	$\mathrm{E}[\mathbf{x}_2(0.2)]$	$\mathrm{StdDev}[\mathbf{x}_1(0.2)]$	$\mathrm{StdDev}[\mathbf{x}_2(0.2)]$
10,000 MC. simulations (data from [15])	387.3	749.5	18.42	10.49
truncated model (19), (22)	387.2	749.6	18.54	10.60

the following simplified version of (19)

$$
\begin{bmatrix}
\dot{\mu}^{(1,0,0)} \\
\dot{\mu}^{(0,1,0)} \\
\dot{\mu}^{(0,0,1)} \\
\dot{\mu}^{(2,0,0)} \\
\dot{\mu}^{(0,2,0)} \\
\dot{\mu}^{(1,1,0)}
\end{bmatrix}
=
\begin{bmatrix}
-c_1+c_2 & 2c_3 & 0 & -c_2 & 0 & 0 \\
-\frac{c_2}{2} & -c_3-c_4 & 0 & \frac{c_2}{2} & 0 & 0 \\
0 & c_4 & 0 & 0 & 0 & 0 \\
c_1 & 0 & 0 & -2c_1+4c_2 & 0 & 4c_3 \\
0 & c_4 & 0 & 0 & -2c_3-2c_4 & -c_2 \\
c_2 & -2c_3 & 0 & -\frac{3c_2}{2} & 2c_3 & -c_1+c_2-c_3-c_4
\end{bmatrix}
\begin{bmatrix}
\mu^{(1,0,0)} \\
\mu^{(0,1,0)} \\
\mu^{(0,0,1)} \\
\mu^{(2,0,0)} \\
\mu^{(0,2,0)} \\
\mu^{(1,1,0)}
\end{bmatrix}
+
\begin{bmatrix}
0 & 0 \\
0 & 0 \\
0 & 0 \\
-2c_2 & 0 \\
0 & c_2 \\
\frac{c_2}{2} & -c_2
\end{bmatrix}
\bar{\mu},
\qquad (21)
$$

where now $\bar{\mu} := \begin{bmatrix} \mu^{(3,0,0)} & \mu^{(2,1,0)} \end{bmatrix}'$ evolves according to

$$
\dot{\mu}^{(3,0,0)} = 3c_1\mu^{(2,0,0)} + (-3c_1+3c_2)\mu^{(3,0,0)} + 6c_3\mu^{(2,1,0)} - 3c_2\mu^{(4,0,0)}
$$

$$
\dot{\mu}^{(2,1,0)} = 2c_2\mu^{(2,0,0)} + (c_1-4c_3)\mu^{(1,1,0)} - \frac{5c_2\mu^{(3,0,0)}}{2}
$$

$$
+ (-2c_1+2c_2-c_3-c_4)\mu^{(2,1,0)} + 4c_3\mu^{(1,2,0)} + \frac{c_2\mu^{(4,0,0)}}{2} - 2c_2\mu^{(3,1,0)},
$$

for which condition (14) does hold, allowing us to find a unique solution φ to (12) and (13), resulting in a truncated system given by (19) and

$$
\bar{\mu} = \varphi(\mu) = \left[\left(\frac{\mu^{(2,0,0)}}{\mu^{(1,0,0)}} \right)^3, \quad \frac{\mu^{(2,0,0)}}{\mu^{(0,1,0)}} \left(\frac{\mu^{(1,1,0)}}{\mu^{(1,0,0)}} \right)^2 \right]'.
\qquad (22)
$$

We perform simulations for both large and small initial populations. Figures 2 and 3 show a comparison between Monte Carlo simulations and the truncated model (19), (22). The coefficients used were taken from [15, Example 1]: $c_1 = 1$, $c_2 = 10$, $c_3 = 1000$, $c_4 = 10^{-1}$. In Fig. 2(a) we used the same initial conditions as in [15, Example 1]:

$$
\mathbf{x}_1(0) = 400, \qquad\qquad \mathbf{x}_2(0) = 798, \qquad\qquad \mathbf{x}_3(0) = 0.
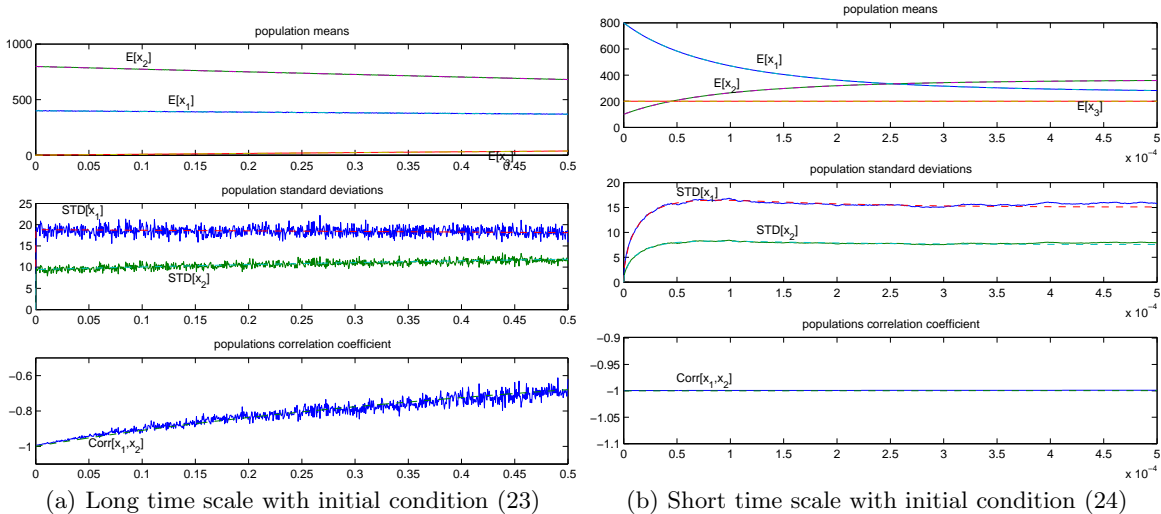\qquad (23)
$$

The match is very accurate, as can be confirmed from Table 3. The values of the parameters chosen result in a pSHS with two distinct time scales, which makes this pSHS computationally difficult to simulate ("stiff" in the terminology of [15]). The initial conditions (23) start in the "slow manifold" $\mathbf{x}_2 = \frac{5}{1000}\mathbf{x}_1(\mathbf{x}_1-1)$ and Fig. 2(a) essentially shows the evolution of the system on this manifold. Figure 2(b) zooms in on the interval $[0, 5 \times 10^{-4}]$ and shows the evolution of the system towards the manifold when it starts away from it at

$$
\mathbf{x}_1(0) = 800, \qquad\qquad \mathbf{x}_2(0) = 100, \qquad\qquad \mathbf{x}_3(0) = 200.
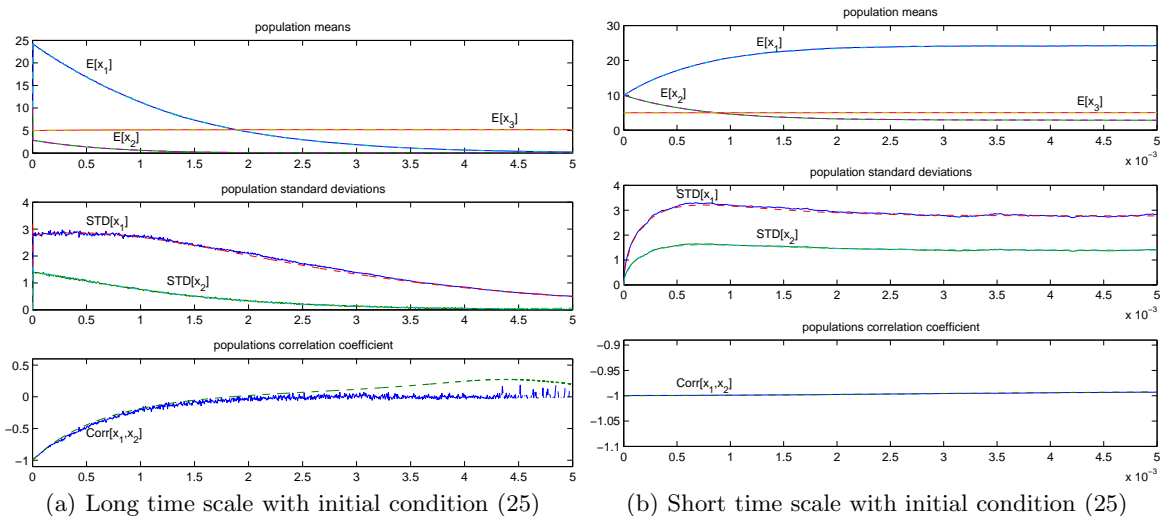\qquad (24)
$$

Figure 3 shows another simulation of the same reactions but for much smaller initial populations:

$$
\mathbf{x}_1(0) = 10, \qquad\qquad \mathbf{x}_2(0) = 10, \qquad\qquad \mathbf{x}_3(0) = 5.
\qquad (25)
$$

The truncated model still provides an extremely good approximation, with significant error only in the covariance between $\mathbf{x}_1$ and $\mathbf{x}_2$ when the averages and standard deviation of these variables get below one. This happens in spite of having used (21) instead of (20) to compute φ. $\qquad\square$

(a) Long time scale with initial condition (23) (b) Short time scale with initial condition (24)

Fig. 2. Comparison between Monte Carlo simulations (solid lines) and the truncated model (19), (22) (dashed lines) for Example 2 with large populations.

(a) Long time scale with initial condition (25) (b) Short time scale with initial condition (25)

Fig. 3. Comparison between Monte Carlo simulations (solid lines) and the truncated model (19), (22) (dashed lines) for Example 2 with small populations.

Example 3. Consider the following system of chemical reactions:

$$\mathrm{X_1 + X_2} \xrightarrow{\ c\ } \mathrm{X_1}, \qquad\qquad \mathrm{X_1 + X_2} \xrightarrow{\ c\ } \mathrm{X_2},$$

and let $\mathbf{x} := (\mathbf{x}_1, \mathbf{x}_2)$ be the number of molecules for X_1 and X_2, respectively. The deterministic chemical rate equations for this system are given by

$$\dot{\mathbf{x}}_1 = -c\mathbf{x}_1\mathbf{x}_2, \qquad\qquad \dot{\mathbf{x}}_2 = -c\mathbf{x}_1\mathbf{x}_2. \tag{26}$$

Equation (26) does not have a unique equilibrium point, in fact, every vector of the form $(\mathbf{x}_0, 0)$ or $(0, \mathbf{x}_0)$, $\mathbf{x}_0 \in \mathbb{R}$ is an equilibrium point for (26). Because of this, general approximate methods based on local

expansions of the Master equation [7], do not apply. The stochastic dynamics of the number of molecules $\mathbf{x} := (\mathbf{x}_1, \mathbf{x}_2)$ can be described by a SHS with continuous dynamics $\dot{\mathbf{x}} = 0$ and reset maps

$$\mathbf{x} \mapsto \phi_1(\mathbf{x}) := \begin{bmatrix} \mathbf{x}_1 \\ \mathbf{x}_2 - 1 \end{bmatrix}, \qquad\qquad \mathbf{x} \mapsto \phi_2(\mathbf{x}) := \begin{bmatrix} \mathbf{x}_1 - 1 \\ \mathbf{x}_2 \end{bmatrix},$$

with intensities $\lambda_1(\mathbf{x}) := c\mathbf{x}_1\mathbf{x}_2$ and $\lambda_2(\mathbf{x}) := c\mathbf{x}_1\mathbf{x}_2$ respectively. For $\psi^{(m_1,m_2)}(x) = x_1{}^{m_1} x_2{}^{m_2}$, $\forall m_1, m_2 \in \mathbb{N}_{\geq 0}$, it can be verified that (8) can be written as follows:

$$
\begin{bmatrix} \dot{\mu}^{(1,0)} \\ \dot{\mu}^{(0,1)} \\ \dot{\mu}^{(2,0)} \\ \dot{\mu}^{(0,2)} \\ \dot{\mu}^{(1,1)} \end{bmatrix}
=
\begin{bmatrix}
0 & 0 & 0 & 0 & -c \\
0 & 0 & 0 & 0 & -c \\
0 & 0 & 0 & 0 & c \\
0 & 0 & 0 & 0 & c \\
0 & 0 & 0 & 0 & 0
\end{bmatrix}
\begin{bmatrix} \mu^{(1,0)} \\ \mu^{(0,1)} \\ \mu^{(2,0)} \\ \mu^{(0,2)} \\ \mu^{(1,1)} \end{bmatrix}
+
\begin{bmatrix}
0 & 0 \\
0 & 0 \\
-2c & 0 \\
0 & -2c \\
-c & -c
\end{bmatrix}
\bar{\mu},
\tag{27}
$$

where $\bar{\mu} := \begin{bmatrix} \mu^{(2,1)} & \mu^{(1,2)} \end{bmatrix}'$ evolves according to

$$\dot{\mu}^{(2,1)} = -2c\mu^{(2,2)} + c\mu^{(1,2)} - c\mu^{(3,1)}$$
$$\dot{\mu}^{(1,2)} = -2c\mu^{(2,2)} + c\mu^{(2,1)} - c\mu^{(1,3)}.$$

This system satisfies condition (14) and any function φ of the form

$$\bar{\mu} = \varphi(\mu) = \left[\frac{\mu^{(2,0)}}{\left(\mu^{(0,1)}\right)^{\nu_1 - 1}} \left(\frac{\mu^{(1,1)}}{\mu^{(1,0)}} \right)^{\nu_1}, \quad \frac{\mu^{(0,2)}}{\left(\mu^{(1,0)}\right)^{\nu_2 - 1}} \left(\frac{\mu^{(1,1)}}{\mu^{(0,1)}} \right)^{\nu_2} \right]'
\tag{28}$$

satisfies (12) and (13), where ν_1, $\nu_2 \in \mathbb{R}$. Explicit conditions on the stoichiometry of the reaction for which (12) and (13) yield a unique solution for φ will appear in [18]. In order to find a unique function φ we now require (12) to hold for the family of lognormal distribution also. It is straightforward to check that for bivariate lognormal variables $\mathbf{y}$ and $\mathbf{z}$,
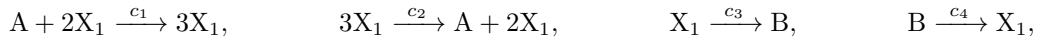
$$E[\mathbf{y}^2 \mathbf{z}] = \frac{E[\mathbf{y}^2]}{E[\mathbf{z}]} \left(\frac{E[\mathbf{y}\mathbf{z}]}{E[\mathbf{y}]} \right)^2,
\tag{29}$$

which corresponds to taking $\nu_1 = \nu_2 = 2$ in (28), and hence, a unique function φ can be found as

$$\bar{\mu} = \varphi(\mu) = \left[\frac{\mu^{(2,0)}}{\mu^{(0,1)}} \left(\frac{\mu^{(1,1)}}{\mu^{(1,0)}} \right)^2, \frac{\mu^{(0,2)}}{\mu^{(1,0)}} \left(\frac{\mu^{(1,1)}}{\mu^{(0,1)}} \right)^2 \right]'.
\tag{30}$$

Figure 4 shows a comparison between Monte Carlo simulations and the truncated model (27), (30) for $c = 5$ and initial conditions, $\mathbf{x}_1(0) = 550$ and $\mathbf{x}_2(0) = 500$. The match is very accurate especially for the mean and standard deviation, as can be seen from the zoomed inserts. $\qquad\square$

Example 4. Consider the Schögl reaction set [16]:

$$A + 2X_1 \xrightarrow{c_1} 3X_1, \qquad 3X_1 \xrightarrow{c_2} A + 2X_1, \qquad X_1 \xrightarrow{c_3} B, \qquad B \xrightarrow{c_4} X_1,$$
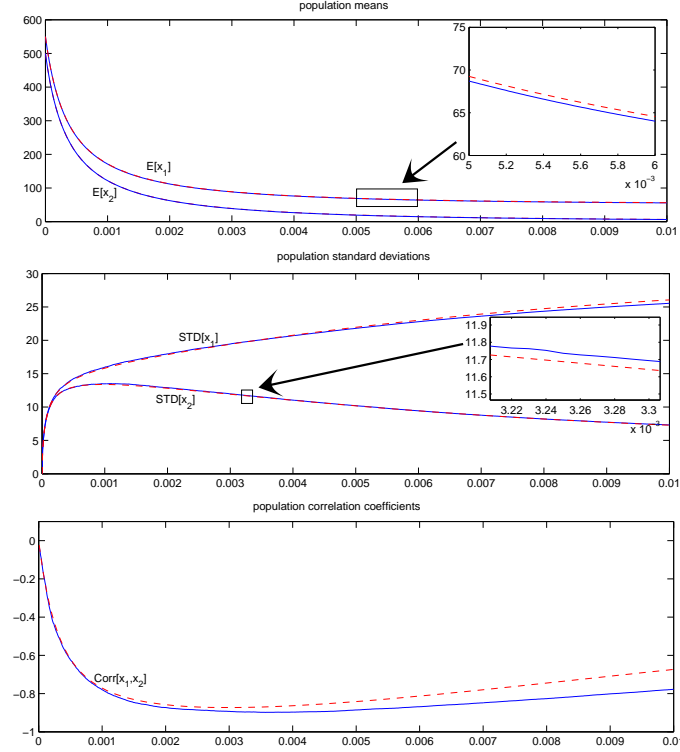
where the number of molecules n_A and n_B of species A and B, respectively, are assumed constants. The deterministic chemical rate equation for this system is

$$\dot{\mathbf{x}} = \frac{c_1}{2} n_A \mathbf{x}^2 - \frac{c_2}{6} \mathbf{x}^3 - c_3 \mathbf{x} + c_4 n_B,
\tag{31}$$

where $\mathbf{x}$ denotes the number of molecules of X_1. This equation has a unique equilibrium point for some values of the coefficients c_i; while it is bistable, for other values (i.e., it has two stable equilibrium points). The evolution of $\mathbf{x}$ can be described by a SHS with continuous dynamics $\dot{\mathbf{x}} = 0$ and reset maps

$$\mathbf{x} \mapsto \phi_1(\mathbf{x}) := \mathbf{x} + 1, \qquad \mathbf{x} \mapsto \phi_2(\mathbf{x}) := \mathbf{x} - 1, \qquad \mathbf{x} \mapsto \phi_3(\mathbf{x}) := \mathbf{x} - 1, \qquad \mathbf{x} \mapsto \phi_4(\mathbf{x}) := \mathbf{x} + 1,$$

Fig. 4. Comparison between Monte Carlo simulations (solid lines) and the truncated model (27), (30) (dashed lines) for Example 3.

with intensities

$$\lambda_1(\mathbf{x}) := \frac{c_1}{2} n_A \mathbf{x}(\mathbf{x} - 1), \qquad \lambda_2(\mathbf{x}) := \frac{c_2}{6} \mathbf{x}(\mathbf{x} - 1)(\mathbf{x} - 2), \qquad \lambda_3(\mathbf{x}) := c_3 \mathbf{x}, \qquad \lambda_4(\mathbf{x}) := c_4 n_B,$$

respectively. For $\psi^{(m)}(x) = x^m$, $\forall m \in \mathbb{N}_{\geq 0}$ we have

$$(L\psi^{(m)})(x) = \frac{c_1}{2} n_A x(x-1)[(x+1)^m - x^m] + \frac{c_2}{6} x(x-1)(x-2)[(x-1)^m - x^m]$$
$$+ c_3 x[(x-1)^m - x^m] + c_4 n_B[(x+1)^m - x^m] \quad (32)$$

and (8) can be written as follows:

$$\begin{bmatrix} \dot{\mu}^{(1)} \\ \dot{\mu}^{(2)} \end{bmatrix} = \begin{bmatrix} -\frac{1}{3} c_2 - \frac{1}{2} n_A c_1 - c_3 & \frac{1}{2} c_2 + \frac{1}{2} n_A c_1 \\ c_3 + 2 n_B c_4 - \frac{1}{2} n_A c_1 + \frac{1}{3} c2 & -\frac{1}{2} n_A c_1 - 2 c_3 - \frac{7}{6} c_2 \end{bmatrix} \begin{bmatrix} \mu^{(1)} \\ \mu^{(2)} \end{bmatrix} + \begin{bmatrix} -\frac{1}{6} c_2 & 0 \\ -\frac{1}{3} c_2 & n_A c_1 + \frac{7}{6} c_2 \end{bmatrix} \bar{\mu} + \begin{bmatrix} n_B c_4 \\ n_B c_4 \end{bmatrix}, \quad (33)$$

where $\bar{\mu} := [\,\mu^{(3)}\;\mu^{(4)}\,]'$ evolves according to

$$\dot{\mu}^{(3)} = -\frac{1}{2} c_2 \mu^{(5)} + (\frac{3}{2} n_A c_1 + 2 c_2) \mu^{(4)} + (-3 c_3 - \frac{8}{3} c_2) \mu^{(3)} + (-n_A c_1 + 3 n_B c_4 + 3 c_3 + \frac{3}{2} c_2) \mu^{(2)}$$
$$+ (-\frac{1}{3} c_2 + 3 n_B c_4 - \frac{1}{2} n_A c_1 - c_3) \mu^{(1)} + n_B c_4$$
$$\dot{\mu}^{(4)} = -\frac{2}{3} c_2 \mu^{(6)} + (2 n_a c_1 + 3 c_2) \mu^{(5)} + (-5 c_2 + n_A c_1 - 4 c_3) \mu^{(4)} + (-n_A c_1 + 4 n_B c_4 + \frac{25}{6} c_2 + 6 c_3) \mu^{(3)}$$

13

$$+ (-\frac{3}{2}n_A c_1 + 6n_b c_4 - 4c_3 - \frac{11}{6}c_2)\mu^{(2)} + (c_3 - \frac{1}{2}n_A c_1 + 4n_B c + \frac{1}{3}c_2)\mu^{(1)} + n_B c_4.$$

Condition (14) is not satisfied, however, if we retain only the two highest powers of x in the right-hand-side of (32), we have the following simplified version of (33)

$$\begin{bmatrix} \dot{\mu}^{(1)} \\ \dot{\mu}^{(2)} \end{bmatrix} = \begin{bmatrix} 0 & \frac{1}{2}c_2 + \frac{1}{2}n_A c_1 \\ 0 & 0 \end{bmatrix} \begin{bmatrix} \mu^{(1)} \\ \mu^{(2)} \end{bmatrix} + \begin{bmatrix} -\frac{1}{6}c_2 & 0 \\ -\frac{1}{3}c_2 & n_A c_1 + \frac{7}{6}c_2 \end{bmatrix} \bar{\mu},$$

where $\bar{\mu} := [\,\mu^{(3)} \; \mu^{(4)}\,]'$ evolves according to

$$\dot{\mu}^{(3)} = -\frac{1}{2}c_2\mu^{(5)} + (\frac{3}{2}n_A c_1 + 2c_2)\mu^{(4)} \qquad \dot{\mu}^{(4)} = -\frac{2}{3}c_2\mu^{(6)} + (2n_a c_1 + 3c_2)\mu^{(5)},$$

for which condition (14) does hold, allowing us to find a unique solution φ to (12) and (13), resulting in a truncated system given by (33) and

$$\bar{\mu} = \varphi(\mu) = \left[\left(\frac{\mu^{(2)}}{\mu^{(1)}} \right)^3, \; \frac{\left(\mu^{(2,0)}\right)^6}{\left(\mu^{(1,0)}\right)^8} \right]'. \tag{35}$$

We perform simulations for two sets of values of coefficients c_i. First, the coefficients are taken as $c_1 = .000002$, $c_2 = .00006$, $c_3 = 10$, $c_4 = 1$, for which (31) has a unique equilibrium point. Figure 5 shows a comparison between Monte Carlo simulations and the truncated model (33), (35) for $\mathbf{x}(0) = 300$ and $n_A = n_B = 1000$.
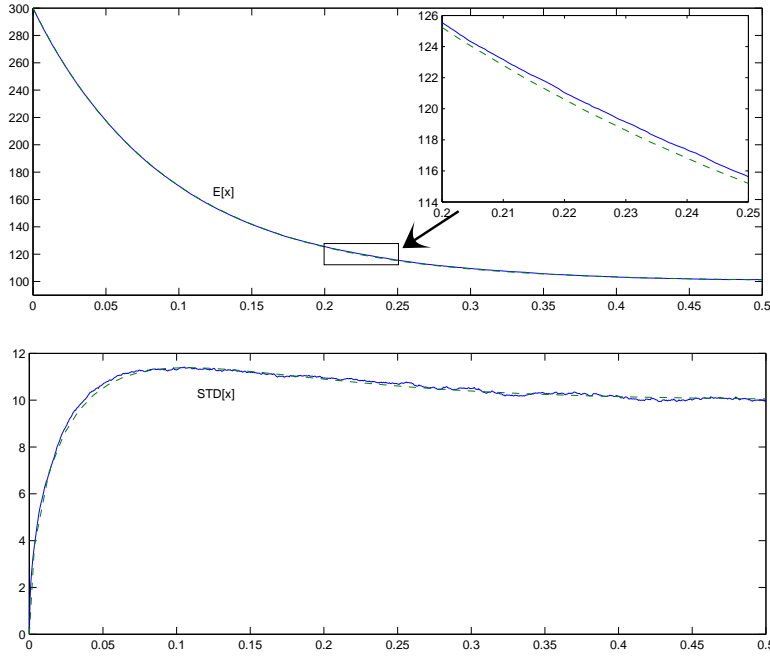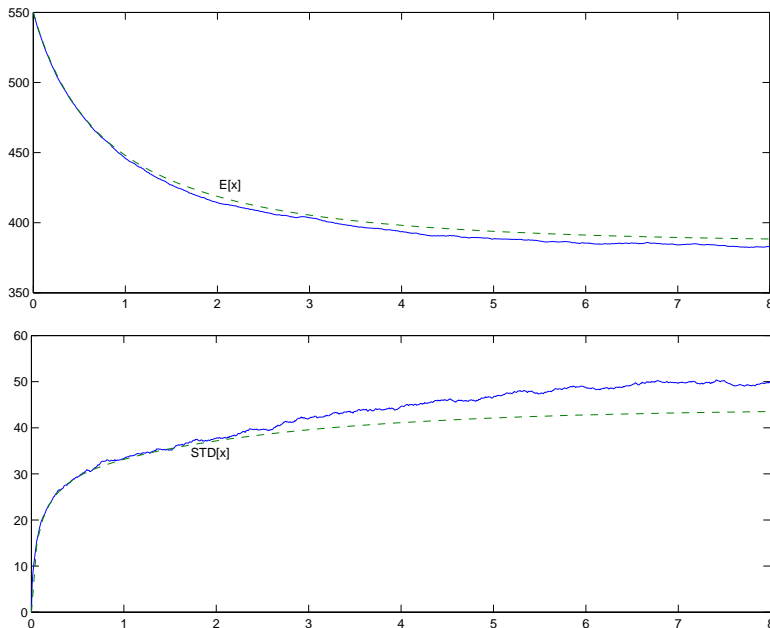

Fig. 5. Comparison between Monte Carlo simulations (solid lines) and the truncated model (33), (35) (dashed lines) for population mean (top) and population standard deviation (bottom) for Example 4, when (31) has a unique equilibrium point.

Next, the coefficients are changed to $c_1 = .000014$, $c_2 = .00006$, $c_3 = 1.4$, $c_4 = .08$, and it can be verified that for these particular values, (31) is bistable. Figure 6 shows a comparison between Monte Carlo

simulations and the truncated model for $\mathbf{x}(0) = 550$ and $n_A = n_B = 1000$. The truncated model provides accurate estimates for times less than one second, with some error after that.

We conjecture that the larger errors observed with the truncated model for this reaction are related to the stoichiometry of this equation with three molecules of X_1 needed for the reaction to take place. This leads to the fact that the dynamics of the mth order moment depend on the $(m+1)^{th}$ and the $(m+2)^{th}$ order moments and therefore the truncation function must provide an estimate of the third and forth order moments based on the first and second. This seems significantly more challenging than just estimating third moments from the first two. Fortunately, stoichiometric coefficients larger than two (as in the Schögl reaction) are not very common. $\square$

Fig. 6. Comparison between Monte Carlo simulations (solid lines) and the truncated model (33), (35) (dashed lines) for population mean (top) and population standard deviation (bottom) for Example 4, when (31) is "bistable."

6 Conclusions and Future Work

An approximate stochastic model for chemically reacting systems was presented in this paper. This was done by representing the population of various species involved in a set of chemical reactions as the continuous state of a pSHS. With such a representation, the dynamics of the infinite vector containing all the statistical moments of the continuous state are governed by an infinite-dimensional linear system of ODEs. We showed that these infinite-dimensional ODEs can be approximated by finite-dimensional nonlinear ordinary differential equations with arbitrary precision and provided a procedure to build this type of approximation. The methodology was illustrate using a variety of examples of chemical reactions that have appeared in literature. By comparison with Monte Carlo algorithms we showed that these approximate stochastic models indeed provided very accurate results.

Several observations arise from these examples, which point to directions for future research:

1. For all the examples considered, it can be seen from equations (17), (22), (28) and (35) that the dependence of $\varphi(\mu)$ on lower-order moments, is as if $\mathbf{x}_i$, is lognormally distributed. As of now we are unable to understand this dependance and further investigation is required.
2. As seen from the examples, the approximate truncated models provide accurate time evolution of lower order moments for the population of species even when the variance is non-zero, i.e., the system has evolved to a "nondeterministic distribution", although the approximate truncated model was constructed assuming a deterministic distribution. As part of our future work we are trying to understand this and develop explicit error bounds when the system evolves to their "nondeterministic distributions".
3. In [19, 20], for infinite-dimensional systems that can be partitioned into a finite-dimensional slow sub-systems and an infinite-dimensional fast one, a finite dimensional system (whose dimension is equal to the slow sub-system) can be obtained, that approximates the solution to the infinite-dimensional system, upto a desired accuracy, for almost all times . Although, the proof of Theorem 2 does not need this kind of structure for the infinite-dimensional system it is possible that in some of the examples something similar might be happening which requires further investigation.
4. The truncated models were constructed by requiring (10) to hold for $N = 2$. A direction of future research consists of constructing approximations based on (10) but for $N > 2$.

Many processes in molecular biology involve a large number of molecular species with very low populations, for which stochastic effect are crucial. Hence, an additional direction for future research is to model stochastic reactions in molecular biology using the techniques presented in this paper.

7   Acknowledgments

Bibliography

[1] McAdams, H.H., Arkin, A.P.: Stochastic mechanisms in gene expression. Proceedings of the National Academy of Sciences U.S.A **94** (1997) 814–819

[2] Arkin, A., Ross, J., McAdams, H.H.: Stochastic kinetic analysis of developmental pathway bifurcation in phage λ-infected *Escherichia coli* cells. Genetics **149** (1998) 1633–1648

[3] Endy, D., Brent, R.: Modelling cellular behaviour. Nature (London) **409** (2001) 391–395

[4] Elowitz, M., Leibler, S.: A synthetic oscillatory netwrok of transcriptional regulators. Nature (London) **403** (2000) 335–338

[5] Gardner, T.S., Cantor, C.R., Collings, J.J.: Construction of a genetic toggle switch in *Escherichia coli*. Nature (London) **403** (2000) 339–342

[6] Walters, M.C., Fiering, S., Eidemiller, J., Magis, W., Groudine, M., Martin, D.I.K.: Enhancers increase the probability but not the level of gene expression. Proceedings of the National Academy of Sciences U.S.A **92** (1995) 7125–7129

[7] Kampen, N.G.V.: Stochastic Processes in Physics and Chemistry. Elsevier Science, Amsterdam, The Netherlands (2001)

[8] Gillespie, D.T.: A general method for numerically simulating the stochastic time evolution of coupled chemical reactions. J. of Computational Physics **22** (1976) 403–434

[9] Gillespie, D.T., Petzold, L.R.: Improved leap-size selection for accelerated stochastic simulation. J. of Chemical Physics **119** (2003) 8229–8234

[10] Gibson, M.A., Bruck, J.: Efficient exact stochastic simulation of chemical systems with many species and many channels. J. of Physical Chemistry A **104** (2000) 1876–1889

[11] Gillespie, D.T.: Approximate accelerated stochastic simulation of chemically reacting systems. J. of Chemical Physics **115** (2001) 1716–1733

[12] Hespanha, J.P.: Stochastic hybrid systems: Applications to communication networks. In Alur, R., Pappas, G.J., eds.: Hybrid Systems: Computation and Control. Number 2993 in Lect. Notes in Comput. Science. Springer-Verlag, Berlin (2004) 387–401

[13] Gunawan, R., Cao, Y., Petzold, L., Doyle, F.J.: Sensitivity analysis of discrete stochastic systems. Biophysical Journal **88** (2005) 2530–2540

[14] McQuarrie, D.A.: Stochastic approach to chemical kinetics. J. of Applied Probability **4** (1967) 413–478

[15] Rathinam, M., Petzold, L.R., Cao, Y., Gillespie, D.T.: Stiffness in stochastic chemically reacting systems: The implicit tau-leaping method. J. of Chemical Physics **119** (2003) 12784–12794

[16] Matheson, I., Walls, D.F., Gardiner, C.W.: Stochastic models of first order nonequilibrium phase transitions in chemical reactions. J. of Statistical Physics **12** (1975) 21–34

[17] Hespanha, J.P.: Polynomial stochastic hybrid systems. In: Hybrid Systems : Computation and Control (HSCC) 2005, Zurich, Switzerland (2005)

[18] Singh, A., Hespanha, J.P.: Models for gene regulatory networks using polynomial stochastic hybrid systems. Submitted (2005)

[19] Chiu, T., D.Christofides, P.: Nonliear control of particulate processes. AIChE J. **45** (1999) 1279–1297

[20] Christofides, P.D., Daoutidis, P.: Finite-dimensional control of parabolic pde systems using approximate inertial manifolds. J. of Math. Anal. Appl. **216** (1997) 398–420